ADVANCED HEALTHCARE MATERIALS
www.advhealthmat.de

Phototuning of Hyaluronic-Acid-Based Hydrogel Properties to Control Network Formation in Human Vascular Endothelial Cells

*Kelum Chamara Manoj Lakmal Elvitigala, Lakshmi Mohan, Wildan Mubarok, and Shinji Sakai**

In vitro network formation by endothelial cells serves as a fundamental model for studies aimed at understanding angiogenesis. The morphogenesis of these cells to form a network is intricately regulated by the mechanical and biochemical properties of the extracellular matrix. Here the effects of modulating these properties in hydrogels derived from phenolated hyaluronic acid (HA-Ph) and phenolated gelatin (Gelatin-Ph) are presented. Visible-light irradiation in the presence of tris(2,2′-bipyridyl)ruthenium(II) chloride hexahydrate and sodium persulfate induces the crosslinking of these polymers, thereby forming a hydrogel and degrading HA-Ph. Human vascular endothelial cells form networks on the hydrogel prepared by visible-light irradiation for 45 min (42 W cm^{-2} at 450 nm) but not on the hydrogels prepared by irradiation for 15, 30, or 60 min. The irradiation time-dependent degradation of HA-Ph and the changes in the mechanical stiffness of the hydrogels, coupled with the expressions of RhoA and β-actin genes and CD44 receptors in the cells, reveal that the network formation is synergistically influenced by the hydrogel stiffness and HA-Ph degradation. These findings highlight the potential of tailoring HA-based hydrogel properties to modulate human vascular endothelial cell responses, which is critical for advancing their application in vascular tissue engineering.

1. Introduction

Understanding the formation of network-like structures of human umbilical vein endothelial cells (HUVECs) is crucial for advancing the knowledge of angiogenesis and its role in various physiological and pathological conditions. This process is necessary for the formation of complex networks of blood vessels and capillaries and plays a crucial role in wound healing, tissue regeneration, and embryonic development. Therefore, exploring the mechanisms of network-like structure formation in vivo and in vitro has become an important area of research in tissue engineering. Kubota et al. first demonstrated in vitro network-like structure formation using a collagen-based gel infused with basement membrane components to determine the role of signals responsible for the morphological differentiation of endothelial cells and network-like structure formation.[1] Recently, hydrogels have emerged as the preferred platform for in vitro angiogenesis, where the polymers used to prepare them are chemically modified to govern both in vitro and in vivo angiogenesis. Although the formation of HUVEC network-like structures is well understood, certain unexplored aspects are being examined using other in vitro models.

Hydrogels have great potential in tissue engineering and regenerative medicine because of their outstanding properties, including their tunable mechanical properties, biocompatibility, and impact on cellular behavior, which is similar to that of the native extracellular matrix (ECM).[2,3] This study focused on modulating the physicochemical properties of hydrogels, such as their stiffness and polymer degradation, to elicit their effects on the network-like structure formation of HUVECs. Natural polymers, such as hyaluronic acid (HA), gelatin, and alginate,[4–6] are widely used to design hydrogels as promising biomimetic materials.[7–9] Alginate is widely utilized owing to its biocompatibility and gelation properties, which are ideal for 3D bioprinting and tissue engineering.[5] Meanwhile, HA and gelatin, the major elements of the basement membrane, have been increasingly employed to fabricate biomaterials because of their biocompatibility,[10] biodegradability, and ability to influence cell behavior, including angiogenesis.[11,12] However, HA alone does not promote

K. C. M. L. Elvitigala, W. Mubarok, S. Sakai
Department of Materials Engineering Science
Graduate School of Engineering Science
Osaka University
Toyonaka, Osaka 560-8531, Japan
E-mail: sakai@cheng.es.osaka-u.ac.jp
L. Mohan
Department of Bioengineering
Henry Samueli School of Engineering
University of California Los Angeles
Los Angeles, CA 90095, USA

The ORCID identification number(s) for the author(s) of this article can be found under https://doi.org/10.1002/adhm.202303787

DOI: 10.1002/adhm.202303787

cellular adhesion; therefore, it must be combined with materials such as gelatin to promote cellular adhesion through the arginine–glycine–aspartic acids (RGD) sequence, and various studies have shown the usefulness of combining HA and gelatin to fabricate biomaterials. In particular, RGD enhances vascular endothelial growth factor (VEGF)-mediated angiogenesis in HA hydrogels by promoting rat sarcoma virus (RAS) pathway activation, a key step for endothelial cell proliferation, migration, and morphogenesis.[13,14] Moreover, the enzymatic responsiveness to matrix metalloproteinases (MMPs) is pivotal, allowing HA-based hydrogels to mimic the dynamic ECM, facilitating cell migration essential for vascular morphogenesis.[15–17]

In addition, the molecular weight of HA, which can be modified by external conditions such as the physical properties of the surrounding biomaterials, can substantially dictate cell response.[18] High-molecular-weight HA (HMWHA) affects cell adhesion and proliferation,[19] whereas low-molecular-weight HA (LMWHA), typically found in degraded ECM, tends to inhibit these processes[20] and instead enhances the network-like structure formation of HUVECs. These effects are primarily mediated by cell surface receptors for HA, such as CD44.[20,21] The interaction between CD44 receptors and HA of different molecular weights results in distinct cellular functions. Specifically, LMWHA fragments play a crucial role in F-actin formation by activating specific signaling pathways.[18] Consequently, F-actin formation induced by LMWHA is a critical factor in regulating the formation of network-like HUVEC structures. Therefore, the controlled degradation of HA during hydrogel preparation, particularly into low-molecular-weight fragments, is important for optimizing the hydrogel properties for vascular tissue engineering.

In our previous studies, we crosslinked phenolated HA (HA-Ph) and phenolated gelatin (Gelatin-Ph) molecules, respectively, with the aid of horseradish peroxidase/hydrogen peroxide (HRP/H_2O_2) to control the physicochemical properties of the resultant hydrogel.[22–24] In HRP-catalyzed gelation, H_2O_2 is used as an electron donor to crosslink phenol (—Ph) groups. Apart from inducing gelation, H_2O_2 is known to cleave the glycosidic bonds of HA through oxidative degradation, which enhances the network-like structure formation of HUVECs on the hydrogel.[22–24] In this study, a photo-crosslinking process was employed to investigate the correlation between the oxidative degradation of HA and the mechanical properties of the hydrogel by evaluating the formation of network-like structure of HUVECs. Typically, the photopolymerization process involves grafting photolabile functional moieties, such as methacryloyl, phenol, or styrene, onto the polymer backbone. Among various photolabile candidates, polymer chains modified with phenol are promising as biomaterials, because their physical properties can be tuned for diverse tissue engineering applications. Therefore, in this study, HA modified with tyramine (Figure S1a, Supporting Information) and gelatin modified with 3-(4-hydroxyphenyl)propionic acid (Figure S1b, Supporting Information) were used to prepare composite hydrogels.

To date, various photoinitiators have been used to crosslink chemically modified polymers. Previously, our group reported the visible-light-mediated crosslinking of various biomaterials, including sugar beet pectin that naturally possessed phenol,[25] as well as Alginate-Ph, HA-Ph, and Gelatin-Ph in which tris(2,2′-bipyridyl)ruthenium(II) chloride hexahydrate ($[Ru(bpy)_3]^{2+}$) was employed as the photoinitiator because of its biocompatibility with living tissues and its ability to initiate crosslinking in a controlled manner without requiring UV light, which can be harmful to cells. When exposed to visible light, HA-Ph and Gelatin-Ph crosslink via radical polymerization in the presence of $[Ru(bpy)_3]^{2+}$ and sodium persulfate (SPS). The crosslinking mechanism of the phenolic moieties can be summarized as follows: $[Ru(bpy)_3]^{2+}$ molecules absorb photons and dissociate SPS into radicals, which then propagate through the phenolic groups, thereby crosslinking the polymer chains by covalently bonding the phenolic moieties in different polymer chains. The novelty of this study lies in the development of an HA-Ph-based hydrogel system by harnessing the power of photo-crosslinking to precisely control the stiffness and oxidative degradation rates of the HA-Ph units. SPS and $[Ru(bpy)_3]^{2+}$ are typically used not only to initiate the crosslinking of polymeric chains by forming SPS radicals but also to contribute to the breakdown of the HA-Ph chains via the oxidative cleavage of glycosidic bonds, leading to a delicate balance between crosslinking and HA-Ph degradation, as illustrated in **Scheme 1**. This balance dictates the overall properties of the hydrogel and subsequently influences the HUVECs' behavior. Previous work by Tzoneva et al. demonstrated the angiogenic potential of endothelial cells in gelatin-based hydrogels through the controlled release of growth factors,[26] while Wang et al. highlighted the benefits of co-delivering growth factors in gelatin hydrogels for enhanced angiogenesis.[27] Yee et al. further explored the stimulation of hyaluronidase in endothelial colony-forming cells via HA-specific receptors, underscoring the importance of HA in vascular network formation.[28] Our study expands on these foundational discoveries by focusing on the generation of LMWHA during hydrogel fabrication, which we have identified as a critical factor in inducing network formation and providing mechanical support for angiogenesis. By offering a substrate that combines both biochemical cues and mechanical properties, our work not only bridges existing gaps but also introduces a comprehensive approach to facilitating angiogenesis, setting a new benchmark for research in tissue engineering and regenerative medicine.

2. Results and Discussion

2.1. Effect of Light Irradiation on Polymer Degradation and Crosslinking

First, the effect of visible-light irradiation on the molecular weight of the sodium salt of HA (Na-HA) was assessed. **Figure 1a,b** reveals that HA treated with the SPS/$[Ru(bpy)_3]^{2+}$ system induced the degradation of HA, as evidenced by a decrease in its viscosity and average molecular weight. As the irradiation time increased, the HA degradation increased because more SPS radicals formed. Reactive oxygen species are known to degrade HA by cleaving the glycosidic bonds between the monomeric units of the HA backbone.[29,30] As shown in Figure 1a, light irradiation time-dependent degradation of Na-HA indicated by decrease in the viscosity of Na-HA solution with increasing light irradiation time. After 15 min of irradiation, the molecular weight of HA decreased from 515 to 417 kDa (Figure 1b). The formation of low-

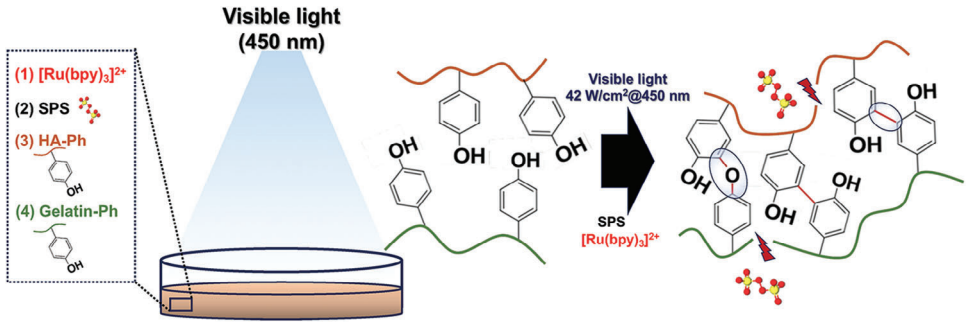

Scheme 1. Schematic illustration of the contradictory impact of SPS on the formation of HA-Ph/Gelatin-Ph hydrogels and the degradation of the crosslinked polymer under visible-light irradiation (450 nm) in the presence of a photoinitiator, $[Ru(bpy)_3]^{2+}$.

molecular-weight fragments increased after 45 min, although the decrease in the average molecular weight of HA was small (Figure 1c). After 60 min, the average molecular weight reached the lowest value of 132 kDa, which was 3.9 times lower than that of nonirradiated HA. Control experiments assessing HA degradation with only light irradiation or SPS treatment alone revealed no significant change in the viscosity and polymer degradation, confirming that the observed HA degradation was specifically mediated by the combined action of light irradiation and the SPS/$[Ru(bpy)_3]^{2+}$ system (Figures S3 and S4, Supporting Information). Therefore, the SPS/$[Ru(bpy)_3]^{2+}$ system is suitable for degrading HA into fragments with a range of molecular weights

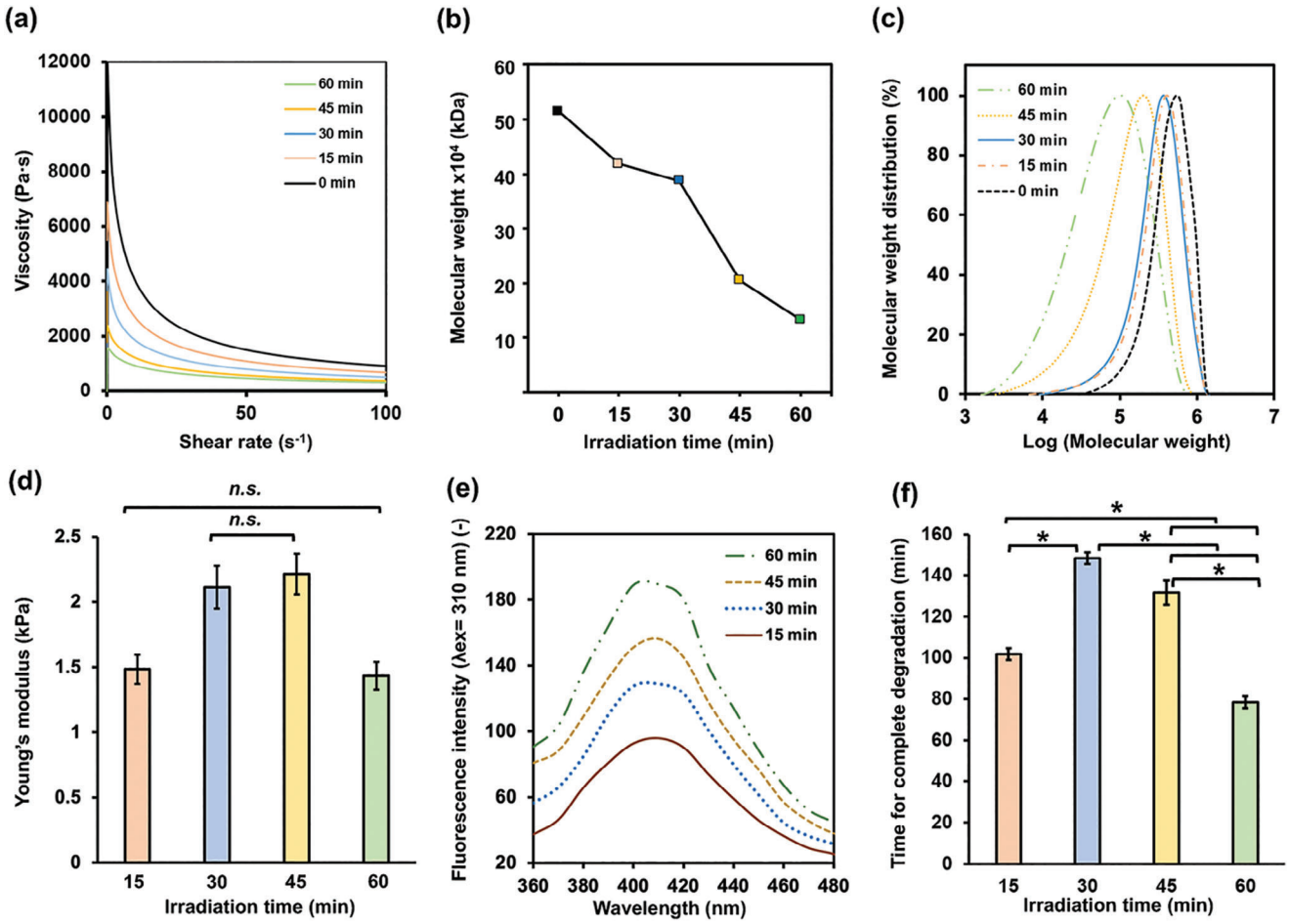

Figure 1. Effect of visible-light irradiation (42 W cm^{-2} at 450 nm) time on the a) viscosity of PBS containing 2 mM SPS, 2 mM $[Ru(bpy)_3]^{2+}$, and Na-HA (2% w/v), b) average molecular weight of Na-HA, c) molecular weight distribution of Na-HA, d) Young's modulus ($n = 5$) of the HA-Ph/Gelatin-Ph hydrogel, and e) diphenol formation in the HA-Ph/Gelatin-Ph hydrogel, f) enzymatic degradation ($n = 3$). Bar: standard error, $^*p < 0.05$, n.s.: no significant difference ($p > 0.05$), Tukey's honestly significant difference (HSD).

simply by changing the visible-light irradiation time (450 nm, 42 W cm^{-2}).

Next, the mechanical properties of the HA-Ph/Gelatin-Ph composite hydrogels prepared through 15–60 min of light irradiation were analyzed. As depicted in Figure 1d, increasing the irradiation time of the HA-Ph/Gelatin-Ph mixture added with SPS/$[Ru(bpy)_3]^{2+}$ from 15 to 30 min significantly increased Young's modulus from 1.5 ± 0.1 to 2.1 ± 0.2 kPa. However, it decreased from 2.2 ± 0.2 to 1.4 ± 0.1 kPa upon further increasing the exposure time from 45 to 60 min. As light irradiation increases, more free radicals are produced by the reaction with SPS, leading to a more robust crosslinked polymer network and thus a stiffer hydrogel. Upon extending the irradiation time to 60 min, however, the hydrogel stiffness decreases because of the significant fragmentation of HA units in the hydrogel. In summary, the HA degradation and hydrogel stiffness analyses indicate that the polymer degradation increases with increasing irradiation time, and the hydrogel stiffness reaches a maximum value and then decreases.

The hydrogel stiffness is maximized upon the optimal fragmentation of HA-Ph during the polymer degradation process. Further, the HA-Ph fragmentation increases with prolonged light irradiation time (Figure 1c), resulting in excessive degradation that decreased stiffness (Figure 1d). To further clarify these phenomena, the change in the degree of crosslinking between HA-Ph and Gelatin-Ph with the irradiation time was analyzed using a fluorescence-based method. As shown in Figure 1e, the formation of diphenol linkages increased as irradiation was prolonged from 15 to 60 min because an increased number of $[Ru(bpy)_3]^{2+}$ molecules were photoexcited, resulting in greater crosslinking of the two polymers. Next, the degradability of the HA-Ph/Gelatin-Ph hydrogel was evaluated by measuring the time required to completely degrade the hydrogel after being treated hyaluronidase and collagenase (Figure 1f; Figure S5, Supporting Information). Consistent with their highest stiffness, the hydrogels obtained by irradiation for 30 and 45 min required the longest times to be degraded (148 and 131 min, respectively), in contrast with the softer hydrogels obtained by 15 and 60 min of light irradiation. Meanwhile, none of the hydrogels obtained by 15–60 min of irradiation degraded after 7 days of immersion in a cell culture medium that did not contain hyaluronidase or collagenase. Our preliminary studies also confirmed that adding 0.1 w/v% Gelatin-Ph did not significantly impact the hydrogel mechanical properties.

2.2. Cell Adhesion and Cell Morphology on the Hydrogel

Understanding the importance of the mechanochemical-property-dependent cell adhesion could reveal the correlation between cellular adhesiveness and the dynamics of the angiogenic behavior of the HUEhT-1 cells (HUVECs immortalized by the electroporation of pIRES-hTERT-hygr). Cell behaviors, such as proliferation, differentiation, and morphology, depend on the physicochemical properties of the substrate.[31–34] As discussed in the previous section, HA-Ph/Gelatin-Ph composite hydrogels with distinct HA-Ph degradation rates and mechanical properties were first produced by modulating visible-light exposure at 450 nm during hydrogel fabrication. Then, the HUEhT-1 cells were cultured on the hydrogels to investigate the effects of their physicochemical properties on the cell morphology, which is an important factor in the promotion or inhibition of angiogenesis. Our findings revealed that the HUEhT-1 cell morphology parameters, particularly the adhesion area and aspect ratio, were significantly influenced by the physicochemical properties of the hydrogel. For the adhesion area, which is the surface area of the substrate covered by cells, significant differences were observed across the hydrogels irradiated for different durations. The hydrogels prepared by 30 and 45 min of irradiation showed the highest average adhesion areas of 4462 and 4373 μm^2, respectively (**Figure 2**a,b), with no significant difference between them. These values are 39% and 23% larger than those of the hydrogels irradiated for 15 and 60 min, respectively; specifically, their adhesion areas were 2740 and 3386 μm^2, respectively. Notably, the cell adhesion areas on the hydrogels were lower than those of the cells cultured directly in the dish (4999 μm^2).

In terms of the aspect ratio, which is a measure of cell elongation and spread on the hydrogel, a steady increase was observed with increasing irradiation time. The lowest aspect ratio of 1.7 was observed in the hydrogel irradiated for 15 min (Figure 2c), and it increased to 2.0, 3.5, and 5.5 (the highest ratio) for the hydrogels irradiated for 30, 45, and 60 min, respectively. These results suggest that the cells spread to a greater extent and become more elongated on the hydrogels prepared with longer irradiation times (Figure 2).

The small adhesion areas of cells on hydrogels with low stiffness are consistent with those observed in our previous studies, wherein HUVECs were circular with a small cell adhesion area on substrates with low stiffness.[23] In addition to the influence of the stiffness of the ECM, the relationship between the cells and ECM materials can influence the cell behavior. According to previous reports, interactions with low-molecular-weight fragments can induce cell elongation.[21] In our earlier study, we observed the same trend with HUVECs and mouse mammary cells cultured on a composite hydrogel (HA-Ph/Gelatin-Ph), in which the cells elongated more in a hydrogel with a higher amount of the LMWHA-Ph fragments.[24] Moreover, the interaction between the LMWHA-Ph fragments and HA receptors, such as CD44 and RHAMM, causes the epithelial–mesenchymal transition (EMT), which is the reprogramming of the epithelial cells into mesenchymal ones.[35] A recent study by Jariyal et al. revealed that LMWHA induces EMT in MCF-7 and MDA-MB-231 cells.[36] Therefore, changes in the aspect ratio of the HUEhT-1 cells cultured in hydrogels prepared with increasing irradiation time can be attributed to both the changes in the substrate stiffness and interactions with the LMWHA-Ph fragments being generated by SPS-mediated degradation.

Exploring cell adhesion dynamics is crucial for understanding HUEhT-1 network formation. As described above, hydrogels irradiated for 30 and 45 min showed the largest average adhesion areas, indicating increased cell spreading. However, the transition from cell spreading to network formation depends on not only the adhesion area but also the cell aspect ratio and the presence of LMWHA-Ph fragments. The aspect ratio suggests more pronounced cell elongation in hydrogels irradiated for longer times. In particular, although both the 30 and 45 min conditions

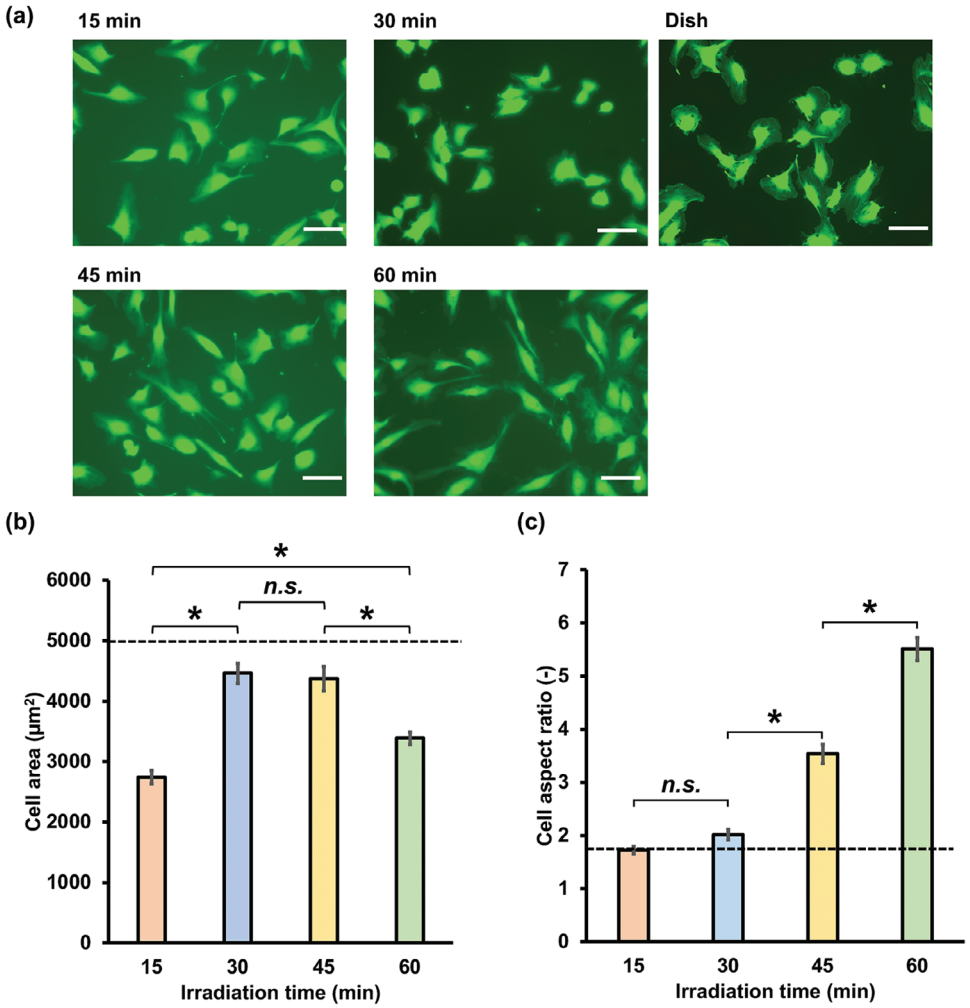

Figure 2. Effect of visible-light irradiation time during hydrogel preparation on the HUEhT-1 cell morphology after 2 days of culture. a) Fluorescence micrographs of the HUEhT-1 cells on hydrogels stained with Calcein-AM. Scale bars: 100 μm. b) Adhesion area and c) aspect ratio of the cells on the hydrogels produced through light irradiation for different durations. Bar: standard error (n= 50). a–c) The dashed lines represent the results of cells cultured in a dish. $^{*}p$ <0.05, n.s.: no significant difference (p > 0.05), Tukey HSD.

promoted cell spreading, the presence of more LMWHA-Ph fragments in the 45 min irradiated hydrogels may be critical in facilitating network formation. These fragments, which are known to interact with HA receptors such as CD44, may induce signaling pathways that support not only cell elongation but also the organization of these elongated cells into network-like structures.

2.3. Network-like Structure Formation

The dependence of the network-like structure formation of HUEhT-1 cells on the visible-light irradiation time of the hydrogel was investigated to further explore the endothelial cell behavior. The HUEhT-1 cells formed a network-like structure on the HA-Ph/Gelatin-Ph hydrogel prepared by 45 min of irradiation (**Figure 3**; Video S1, Supporting Information). HUEhT-1 cells formed a complete network-like structure within 16 h, as shown in Figure 3, which became unstable and disintegrated after 24 h. According to Califano and Reinhart-King,[37] substrate mechanics and matrix chemistry play vital roles in endothelial cell network assembly. The authors reported that soft substrates (0.2–1 kPa) do not promote network formation of endothelial cells, but stiffer substrates (2.5–10 kPa) do.[37] Consistent with a previous study in which the stiffness was in the same range, the hydrogel prepared with 45 min of light irradiation presented a more robust network-like structure of HUEhT-1 cells than the soft hydrogels obtained by 15 and 60 min of light irradiation (Figure 3). Interestingly, the hydrogel obtained after 60 min of light irradiation also supported some network-like structure formation of the HUEhT-1 cells, although it was less distinct than that obtained in the hydrogel formed through 45 min of irradiation (Figure 3). These results indicate that the combined effect of the mechanical properties of the hydrogel and the amount of LMWHA-Ph fragments generated through the degradation of HA-Ph by SPS in the hydrogel irradiated for 45 min caused the

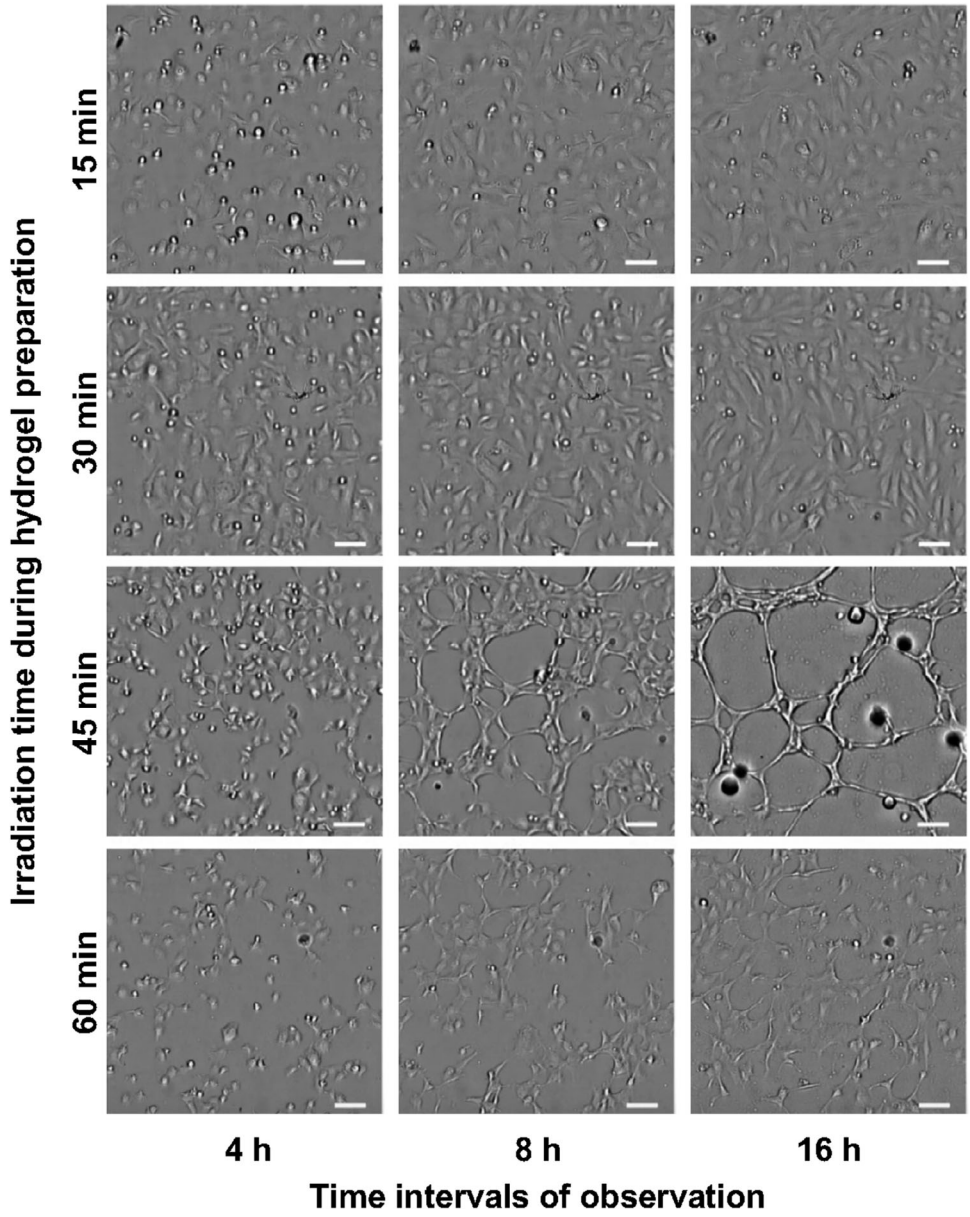

Figure 3. Effect of the visible-light irradiation time on HUEhT-1 cell network formation on HA-Ph/Gelatin-Ph hydrogels obtained through 15–60 min of visible-light irradiation, observed on 4, 8, and 16 h of culture. Scale bar: 100 µm (see Video S1 in the Supporting Information).

formation of a network-like structure of the HUEhT-1 cells. The greater amount of HA-Ph fragments generated during 45 min of irradiation might induce the formation of a more robust network-like structure of the HUEhT-1 cells compared with that achieved with the hydrogel irradiated for 30 min, although both the hydrogels had nearly the same stiffness. In our study, network formation was optimized at a hydrogel stiffness of ≈2.2 kPa, filling a crucial gap in the understanding of the effects of matrix stiffness, as outlined by Frye et al.,[17] Alderfer et al.,[38] Hanjaya-Putra et al.,[39] and Ingber.[40] Collectively, these studies span a range of stiffness values and highlight the importance of mechanical cues in vascular and lymphatic morphogenesis, from promoting cell elongation and sprouting to facilitating attachment and spreading. Considering the stiffness values reported by Hanjaya-Putra et al.,[39] which highlight the influence of substrate mechanics on endothelial progenitor cell tubulogenesis across a range of stiffness from soft (10 Pa) to rigid (650 Pa) matrices, our optimal stiffness of ≈2.2 kPa represent an advance beyond this range. Similarly, Alderfer et al.[38] reported that stiffness values of ≈30 Pa were optimal for lymphatic tube formation, which would underscore the importance of this stiffness range in both vascular and lymphatic endothelial biology and provide a comprehensive understanding of the role of the mechanical environment in both hemangiogenesis and lymph angiogenesis.

A possible mechanism for the network formation of the HUEhT-1 cells on the hydrogel obtained with 45 min of light irradiation could be explained by the interactions of the LMWHA-Ph fragments in the hydrogel with CD44 and RHAMM receptors,

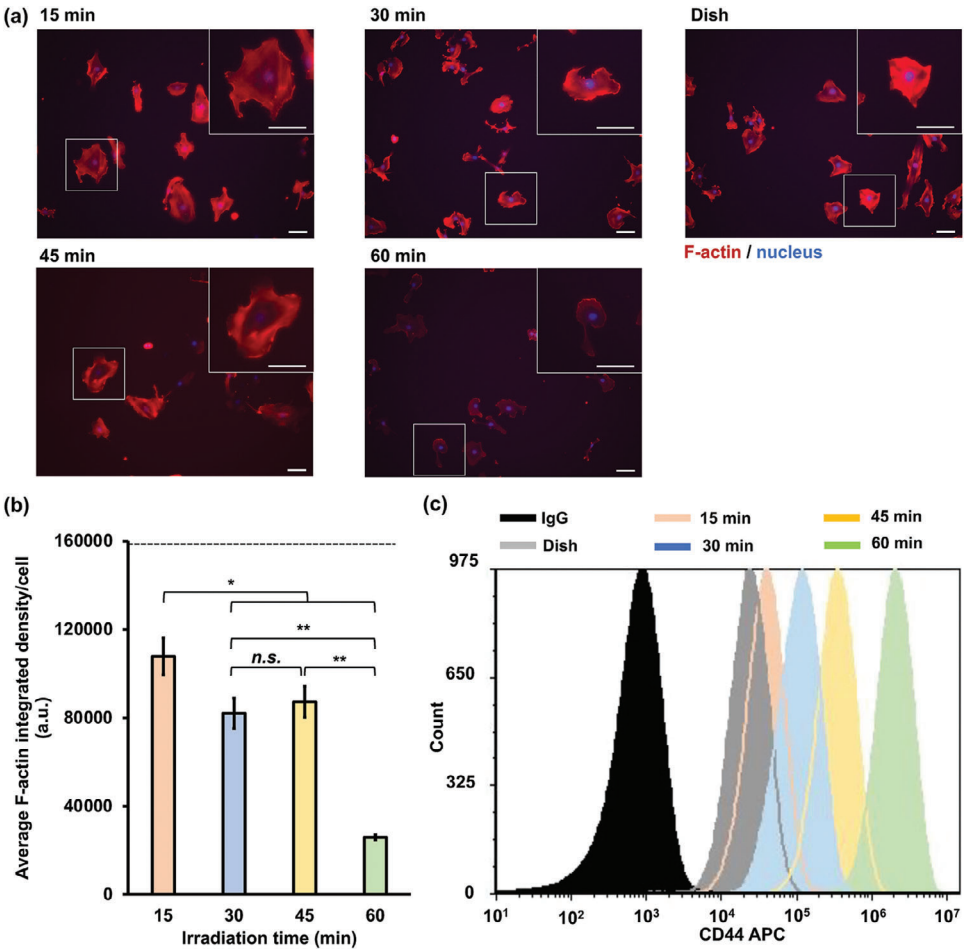

Figure 4. F-actin formation in HUEhT-1 cells cultured on HA-Ph/Gelatin-Ph hydrogels obtained through irradiation for 15, 30, 45, and 60 min. a) Fluorescence microscopic images obtained by a fluorescence microscope and b) integrated density of the F-actin in HUEhT-1 cells cultured in a dish (dashed line) and on different hydrogels. c) Flow cytometry histogram of allophycocyanin (APC) in cells cultured on each hydrogel and dish. Scale bars: 100 µm. Bar: standard error ($n = 50$ cells). *$p < 0.05$, **$p < 0.005$, n.s.: no significant difference ($p > 0.05$), Tukey HSD.

which promote network-like structure formation, as reported earlier.[27,41] These receptors induce the formation of network-like structures of the HUEhT-1 cells through distinct pathways. The interaction between HA with CD44 could activate γ-adduct formation, while that between HA and RHAMM induces AP-1 binding to the RHAMM promoter, thereby inducing the network-like structure formation of the cells.[42,43]

2.4. Role of F-actin and CD44

F-actin formation during network formation is crucial for the establishment and maintenance of the network structure. A previous study by Choi et al. reported the importance of F-actin expression and assembly in promoting endothelial cell migration and angiogenesis.[44] Other studies have also demonstrated that cytoskeletal reorganization, which is the primary step in angiogenesis, is critical for the migration of HUVECs. Furthermore, the interaction of ECM materials with relevant cell surface receptors, such as CD44 and RHAMM, initiates intracellular signaling pathways, leading to F-actin formation,[45] and these events ultimately promote or inhibit angiogenesis. Therefore, the hydrogel-stiffness-dependent and HA-Ph-CD44 interaction-related F-actin organization in the HUEhT-1 cells was examined by staining the actin stress fibers in the cells (**Figures 4** and **5**). The cells cultured on the hydrogel obtained with 60 min of light irradiation showed the lowest amount of stress fibers among the different hydrogels. However, the cells cultured on the hydrogel irradiated for 15 min showed the highest integrated density of stress fibers, whereas those cultured on the hydrogels irradiated for 30 and 45 min showed no significant difference in actin fiber formation (Figure 4b). The cells cultured in the dish showed the highest integrated density, confirming the formation of more stress fibers. The stiffness-dependent F-actin formation could be explained based on mechanotransduction. HA is known to exert different modulatory effects on CD44 receptors according to its molecular weight. The interaction of LMWHA-Ph with CD44 receptors has been recognized to play a significant role in cell adhesion and intracellular signaling pathways. Specifically, a high F-actin content enhances cell adhesion to the hydrogel, potentially leading to a less conducive environment for network formation. On the other hand, flow cytometry results showed the opposite

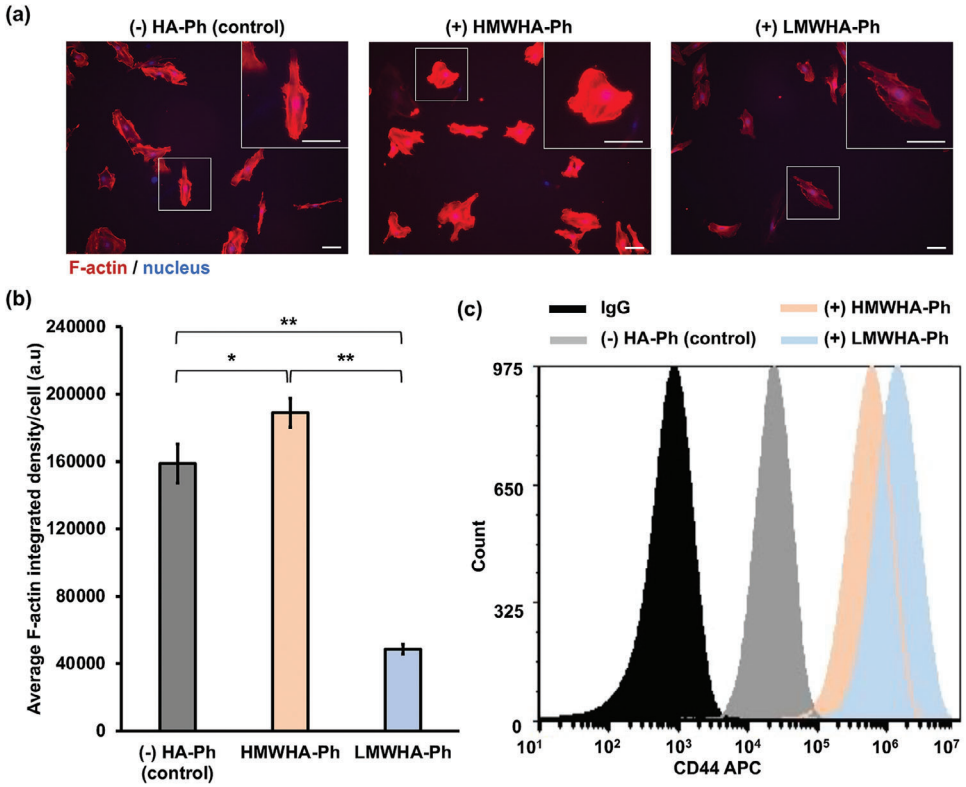

Figure 5. a) Fluorescence observation of F-actin formation in HUEhT-1 cells cultured on a well plate treated with HMWHA-Ph and LMWHA-Ph. Cells cultured in an untreated dish (without HA-Ph treatment) were used as control. Scale bar: 100 μm. b) Integrated density of F-actin under each condition. c) Flow cytometry histogram of the APC in cells cultured in the presence and absence of different HA-Ph fragments. Bar: standard error ($n = 50$ cells). $*p < 0.05$, $**p < 0.005$, Tukey HSD.

trend in F-actin formation with increasing irradiation time, as shown in Figure 4c.

As mentioned above, when the irradiation time was increased, more LMWHA-Ph fragments were generated, which may have enhanced CD44 expression. This increase in CD44 expression by LMWHA-Ph fragments initiates CD44-mediated intracellular signaling pathways related to F-actin formation. Moreover, Kim and Owen suggested that the interaction between LMWHA and CD44 receptors enhances the activation of CD44 receptors and eventually facilitates network formation.[46] Intriguingly, while F-actin formation was notably higher in hydrogels prepared by 15 and 30 min of irradiation, a robust cell network was formed in the hydrogel prepared by 45 min of irradiation. These contradictory results can be attributed to the intricate relationships among F-actin expression, CD44 expression, and substrate stiffness.

To further elucidate the effect of the interaction between HA-Ph and CD44 on F-actin formation and CD44 expression, additional experiments were conducted (Figure 5). Cells were cultured in a cell culture dish treated with HMWHA-Ph or LMWHA-Ph using the growth medium. Compared with the cells cultured in an untreated dish, the cells in the LMWHA-Ph-treated dish showed less F-actin formation, whereas the cells cultured in the dish treated with HMWHA-Ph showed more F-actin formation. This observation suggests that LMWHA-Ph may affect cell adhesion or spreading, possibly because of its smaller size and possible differences in interactions with cell surface receptors compared with HMWHA-Ph. Further, the higher integrated density of F-actin for the cells in the dish treated with HMWHA-Ph compared with that in the untreated dish (Figure 5b) could be the result of improved cell adhesion or spreading owing to the interaction of the larger HMWHA-Ph molecules with cell surface receptors, which may influence cell behavior and lead to a more robust F-actin cytoskeleton. Contrarily, flow cytometry results revealed a different trend. Specifically, when LMWHA-Ph interacted with the HUEhT-1 cells, CD44 expression levels increased (Figure 5c). This interaction led lower F-actin formation, especially when compared to the effects of HMWHA-Ph.

To elucidate the mechanism by which LMWHA-Ph affects F-actin formation via CD44 receptors, additional experiments were conducted (**Figure 6**). The CD44 receptor was blocked with an anti-CD44 antibody, and the cells were cultured in a cell culture dish with an LMWHA-Ph-treated medium. The results provided critical insights into the role of CD44 in mediating the effects of LMWHA-Ph on the cell behavior (Figure 6). Specifically, the cells cultured with LMWHA-Ph, under CD44-blocking conditions ((+) CD44 antibody), showed no significant differences from the control in terms of their aspect ratio and the integrated density of F-actin. This result suggests that CD44 blockade effectively mitigated the LMWHA-Ph-induced changes in cell elongation and F-actin rearrangement observed in the absence of blockade. In

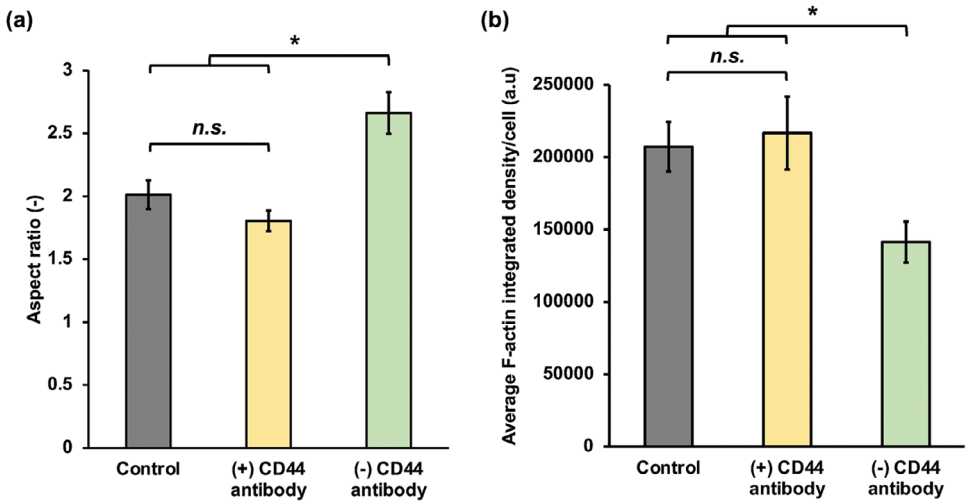

Figure 6. Effect of the CD44 receptor and LMWHA-Ph interaction on the a) aspect ratio and b) F-actin formation in HUEhT-1 cells cultured in a dish using a medium containing LMWHA-Ph with CD44 receptors blocked and not blocked. Bar: standard error ($n > 20$ cells). *$p < 0.05$, n.s.: no significant difference ($p > 0.05$), Tukey HSD.

contrast, cells cultured with LMWHA-Ph without CD44 receptor blocking exhibited a large aspect ratio and decreased integrated density of F-actin. Considered together, these results strongly suggest that CD44 plays a key role in mediating the effects of LMWHA-Ph on F-actin rearrangement and cell shape changes. The blockade of the CD44 receptors effectively negated the effect of LMWHA-Ph, providing substantial evidence that LMWHA-Ph-induced changes were regulated, at least in part, through interactions with the CD44 receptors.

2.5. Role of RhoA and β-actin on F-actin Formation

The formation of F-actin fibers plays a crucial role in HUEhT-1 cell network formation, especially through interactions between LMWHA-Ph fragments and CD44 receptors. As discussed in previous sections, the interaction of LMWHA-Ph with CD44 receptors may result in the modulation of the signaling pathways that are critical for the production of F-actin fibers. RhoA stimulates the formation of stress fibers, and β-actin is one of the primary proteins involved in the regeneration of F-actin fibers. Therefore, the irradiation time-dependent RhoA and β-actin gene expression levels are discussed in this section. According to the findings shown in **Figure 7**, compared with the gene expression of the cells cultured in untreated cell culture dishes, the cells cultured on the hydrogel prepared with 30 min of light irradiation showed the highest levels of RhoA and β-actin gene expression of 1.26 and 1.36, respectively. The hydrogels obtained through 45 and 60 min of irradiation showed the lowest expression of both genes, as shown in Figure 7. Notably, different irradiation times induced changes in the expression of genes related to F-actin formation. Thus, the intricate effects of light irradiation on

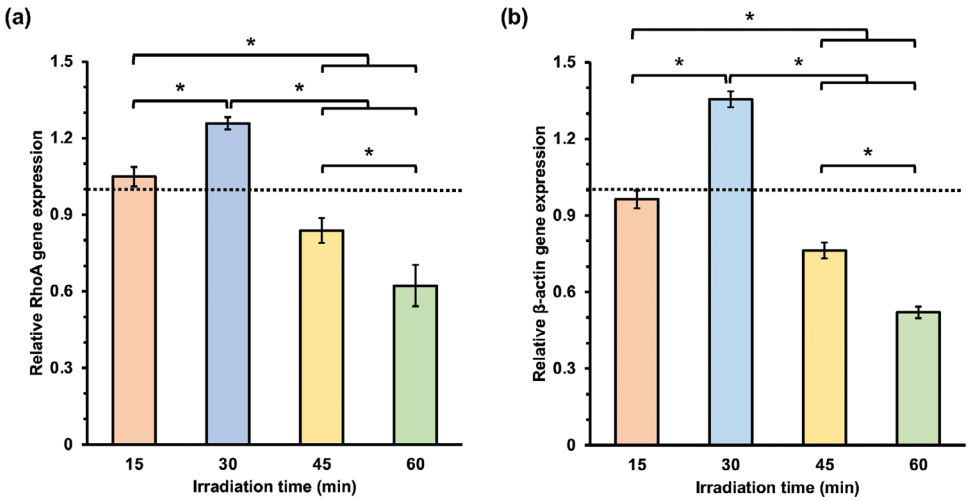

Figure 7. Effect of light irradiation time on relative a) RhoA expression and b) β-actin expression of HUEhT-1 cells cultured on HA-Ph/Gelatin-Ph hydrogels obtained through irradiation for 15, 30, 45, and 60 min with respect to cells cultured in a dish (dashed line). Bar: standard error ($n = 2$). *$p <$ 0.05, Tukey HSD.

LMWHA-Ph fragmentation and CD44 receptor interactions play a critical role in modulating F-actin dynamics. Future research should further optimize these parameters for targeted outcomes in specific signaling pathways related to network-like structure formation of cells.

3. Conclusion

This study investigated the role of hydrogel constitution, with particular emphasis on the effect of photo-crosslinking, and the effects of the mechanical and chemical properties of the hydrogel on HUEhT-1 cell behavior. By tuning the visible-light irradiation time during hydrogel preparation, variations in HA-Ph degradation rates and the associated hydrogel stiffness were detected. HUEhT-1 cells exhibited distinct behaviors depending on the level of HA-Ph degradation and hydrogel stiffness. The HUEhT-1 cells cultured in the hydrogel with intermediate stiffness prepared through prolonged light irradiation exhibited optimal elongation and network formation, suggesting an interplay between the degree of HA-Ph degradation and substrate stiffness. This study focused on the interactions between the HA-Ph and CD44 receptors and their effect on HUEhT-1 cellular function. Notably, other hyaluronan receptors, such as RHAMM, might govern the HUEhT-1 cellular functions through interactions with HA-Ph. Therefore, the role of other hyaluronan receptors on the HUEhT-1 cellular functions will be considered in our future studies. These findings highlight the dynamic relationship between the HA-Ph degradation rate and hydrogel stiffness. Therefore, understanding these interactions provides a promising avenue for improving the biofabrication of vascularized tissues and advancing in vitro endothelial cell studies.

4. Experimental Section

Materials: HA-Ph with four phenyl groups per 100 repeating units of HA and Gelatin-Ph with a phenyl content of 4.1 × 10^{-4} mol g^{-1} were synthesized according to previously reported methods.[47,48] In brief, tyramine hydrochloride (Chem-Impex, Wood Dale, IL, USA) was reacted with Na-HA (Kewpie, Tokyo, Japan) to obtain HA-Ph, as shown in Figure S1a (Supporting Information). In addition, type B gelatin from bovine skin (Sigma–Aldrich, St. Louis, MO, USA) was modified with 3-(4-hydroxyphenyl)propionic acid (Tokyo Chemical Industry, Tokyo, Japan) to obtain Gelatin-Ph, as shown in Figure S1b (Supporting Information). The introduction of phenolic groups into HA and gelatin was confirmed through ^{1}H NMR spectroscopy (Figure S2, Supporting Information). SPS, phosphate-buffered saline (PBS) containing 4% w/w paraformaldehyde, and hyaluronidase from ovine testes (1110 U mL^{-1}) were purchased from FUJIFILM Wako Pure Chemical (Osaka, Japan). $[Ru(bpy)_3]^{2+}$ was purchased from Tokyo Chemical Industry (Tokyo, Japan). Phalloidin-iFluor 647 (ab176759) and 488 (ab176753) were procured from Abcam (Cambridge, UK).

Cell Culture: HUVECs immortalized by the electroporation of pIRES-hTERT-hygr (HUEhT-1) cell line were purchased from RIKEN Cell Bank (Ibaraki, Japan). Cell culture medium, MCDB107 (Nissui, Tokyo, Japan), supplemented with 10 ng mL^{-1} endothelial growth factor, basic fibroblast growth factor (Sigma–Aldrich, St. Louis, MO, USA), and 10% (v/v) fetal bovine serum (FBS) was used to maintain the culture. The cell culture environment was maintained at 37 °C in a humidified incubator with 5% CO_2.

Rheological Properties and Molecular Weights of Polymers: Sodium salt of HA (Na-HA, 2% w/v) was dissolved in PBS containing SPS and $[Ru(bpy)_3]^{2+}$ at a final concentration of 2 mM each and then exposed to 450 nm light for 15, 30, 45, or 60 min at an intensity of 42 W cm^{-2}. The viscoelastic properties of the polymer solutions were determined using a parallel plate rheometer (HAAKE MARS III, Thermo Fisher Scientific, MA, USA) at 1% constant shear strain and a 1 mm gap between plates at 25 °C. The molecular weight of Na-HA was analyzed by high-performance liquid chromatography (Shimadzu, Kyoto, Japan). Pullulan standards were used to prepare a calibration curve for determining the molecular weight of each sample.

Hydrogel Preparation: Composite hydrogels were prepared by photo-crosslinking HA-Ph and Gelatin-Ph. Gelatin-Ph was used to enhance cellular adhesion because of the poor cell adhesion properties of HA-Ph (Figure S7, Supporting Information). A mixed solution of HA-Ph (2% w/v), Gelatin-Ph (0.1% w/v), SPS (2 mM), and $[Ru(bpy)_3]^{2+}$ (2 mM) was prepared in PBS and exposed to 450 nm light (42 W cm^{-2}) for 15, 30, 45, or 60 min. The SPS and concentrations were chosen according to the previous studies.[25,49]

Hydrogel Stiffness: Hydrogel sheets with a diameter of 35 mm and a thickness of 2 mm were prepared in a 35 mm dish, as described in the "Hydrogel Preparation" section. Specifically, 1 mL of the polymer solution was used per dish. The Young's moduli of the hydrogels were measured using a material tester (EZ-SX; Shimadzu, Kyoto, Japan). The hydrogel sheets were compressed at the rate of 6.0 mm min^{-1} using a 5 mm diameter probe at 37 °C. The stress–strain curves obtained at 1–10% compression were used to calculate the Young's moduli.

Hydrogel Degradation: Hydrogel pellets with a diameter of 8 mm and a thickness of 2 mm were prepared, as described in the "Hydrogel Preparation" section. Unreacted materials in the hydrogels were removed by washing several times with PBS. Then, the hydrogel pellets were soaked in a mixture of collagenase and hyaluronidase (both at a final concentration of 0.1 w/v%) in an MCDB107 medium at 37 °C. Next, changes in the hydrogel morphology over time and the time required for the hydrogel to degrade were evaluated from photographs taken at appropriate time intervals.

Fluorescence-Based Evaluation of Phenol Crosslinking: The hydrogel was prepared as described in the "Hydrogel Preparation" section in a 96-well plate by pouring 200 µL of the polymer and photo-crosslinker solution into each well. The influence of light irradiation time (15–60 min) on the coupling of the phenol groups attached to the polymer backbone was determined using a fluorescence plate reader (Gemini XPS; Molecular Devices, San Jose, CA, USA). The fluorescence intensity between 350 and 500 nm was measured under 310 nm excitation.

Cell Adhesion and Morphology: The hydrogel was fabricated in a 6-well plate by adding 1 mL of the polymer and photo-crosslinker solution into each well. Before cell seeding, unreacted materials in the hydrogels were removed by washing several times with PBS. The viability of the HUEhT-1 cells cultured on this hydrogel was determined using a previously reported method.[50] At the concentrations used in this study, SPS and $[Ru(bpy)_3]^{2+}$ showed no toxic effects in cells (Figure S6, Supporting Information), consistent with the previous report.[25] Subsequently, the hydrogels were replenished with fresh MCDB107 medium, and then, HUEhT-1 cells were seeded onto the hydrogels (5.0 × 10^3 cells cm^{-2}). After 2 days of culture, the cell adhesion area and cell shape changes (quantified as the aspect ratio, i.e., the major axis to the minor axis of the fitted ellipse representing each cell) were analyzed by staining with Calcein-AM (Dojindo, Kumamoto, Japan). The fluorescently stained cells were imaged using a fluorescence microscope (BZ-9000; Keyence, Osaka, Japan). The cell adhesion area and aspect ratio were measured using ImageJ software (version 2.1.0/1.53c, NIH, Bethesda, MO, USA).

Network-like Structure Formation: The HA-Ph/Gelatin-Ph hydrogels were prepared in a 6-well plate and washed several times with PBS to remove the unreacted materials. Thereafter, HUEhT-1 cells with 70% confluence (through passage number 18) were trypsinized and seeded onto the hydrogel in each well at 4.0 × 10^4 cells cm^{-2} in low-serum (2% v/v FBS) MCDB107 medium. The network-like structure formation of the cells was analyzed using an inverted light microscope (CKX41; Olympus, Tokyo, Japan) and Provi CM20 incubation monitoring system (Olympus, Tokyo, Japan) from 4 to 16 h post culture.

F-actin Formation: Actin fiber rearrangement in the HUEhT-1 cells was analyzed as reported previously.[24] Briefly, cells were fixed using PBS containing 4% (w/w) paraformaldehyde for 30 min and permeabilized by adding 4-(2-hydroxyethyl)-1-piperazineethanesulfonic acid buffer (pH 5.5) containing 1% (v/v) bovine serum albumin (BSA). Next, the cells were stained using CytoPainter Phalloidin-iFluor 647 or 488 reagent (1×) and then washed thrice with PBS after staining. Subsequently, the cells were stained with 4′,6-diamidino-2-phenylindole (DAPI) to identify the cell nuclei based on a previously reported method.[22] The fluorescence intensity of the captured images was measured using ImageJ software. Finally, the integrated density, defined as the sum of all the intensities in the pixels of the selected area, was calculated.

Flow Cytometry: After 48 h of culture, the cells were carefully detached from the hydrogel by treatment with hyaluronidase 0.1% w/v) for 10 min. They were then incubated with the BD FC block reagent (BD Biosciences, San Jose, CA, USA) to block nonspecific binding sites. Subsequently, the cells were washed with PBS and incubated with an allophycocyanin (APC)-conjugated mouse CD44 antibody (EXBIO Praha, a.s., Nad Safinou, Czech Republic) for 30 min at 4 °C. Thereafter, the cells were washed twice with PBS and analyzed using a BD Accuri C6 flow cytometer (BD Biosciences, San Jose, CA, USA).

Real-Time Quantitative Polymerase Chain Reaction Analysis for β-actin and RhoA Expression: The HUEhT-1 cells were collected from the hydrogel after treatment with hyaluronidase (1 mg mL^{-1}) for 10 min. The cells cultured in cell culture dishes were trypsinized and subjected to RNA extraction. The total RNA was isolated from the cultured HUEhT-1 cells using an RNA isolation kit (Takara, Shiga, Japan), following the manufacturer's protocol. Reverse transcription was performed using the PrimerScript RT Master Mix reagent kit, following the manufacturer's protocol (Takara, Shiga, Japan). The RhoA and β-actin genes were detected by quantitative polymerase chain reaction (qPCR) using the TB Green Master Kit (Takara, Shiga, Japan). Quantification was performed via the comparative $C(t)$ method using glyceraldehyde-3-phosphate dehydrogenase (GAPDH) as the housekeeping gene.

Statistical Analysis: Microsoft Excel 2019, version 1808 (Microsoft Corp., Redmond, WA, USA) was used for the statistical data analysis. One-way analysis of variance (ANOVA) was used to determine statistical differences between the results obtained under each experimental condition. Significant differences were determined based on post-hoc t-test using Tukey's honestly significant difference (HSD), in which $p < 0.05$ was considered significantly different.

Supporting Information

Supporting Information is available from the Wiley Online Library or from the author.

Acknowledgements

This study was supported by Toyota Physical and Chemical Research Institute, the Japan Society for the Promotion of Science (JSPS) Fostering Joint International Research (B) (Grant No. 20KK0112), and a Grant-in-Aid for JSPS Fellows No. 22F22373. W.M. was supported by a JSPS Postdoctoral Fellowship in Japan. The authors would like to thank Editage (www.editage.com) for English language editing. The graphical abstract was made using BioRender.

Conflict of Interest

The authors declare no conflict of interest.

Data Availability Statement

The data that support the findings of this study are available from the corresponding author upon reasonable request.

Keywords

composite hydrogel, degradation, HUVEC, hyaluronic acid, photo-crosslinking

Received: October 31, 2023
Revised: March 6, 2024
Published online:

[1] Y. Kubota, H. K. Kleinman, G. R. Martin, T. J. Lawley, *J. Cell Biol.* **1988**, *107*, 1589.
[2] K. Chwalek, L. J. Bray, C. Werner, *Adv. Drug Delivery Rev.* **2014**, *79*, 30.
[3] M. V. Tsurkan, P. V. Hauser, A. Zieris, R. Carvalhosa, B. Bussolati, U. Freudenberg, G. Camussi, C. Werner, *J. Controlled Release* **2013**, *167*, 248.
[4] X. Chen, H. Zhang, J. Cui, Y. Wang, M. Li, J. Zhang, C. Wang, Z. Liu, Q. Wei, *Gels* **2023**, *9*, 155.
[5] J. Zhang, Y. Wang, Q. Wei, Y. Wang, M. Li, D. Li, L. Zhang, *Int. J. Biol. Macromol.* **2022**, *219*, 1216.
[6] J. Zhang, Y. Wang, Q. Wei, M. Li, X. Chen, *J. Colloid Interface Sci.* **2024**, *653*, 1514.
[7] F. Fan, B. Su, A. Kolodychak, E. Ekwueme, L. Alderfer, S. Saha, M. J. Webber, D. Hanjaya-Putra, *ACS Appl. Mater. Interfaces* **2023**, *15*, 58195.
[8] G. Camci-Unal, D. Cuttica, N. Annabi, D. Demarchi, A. Khademhosseini, *Biomacromolecules* **2013**, *14*, 1085.
[9] D. Jiang, J. Liang, P. W. Noble, *Annu. Rev. Cell Dev. Biol.* **2007**, *23*, 435.
[10] S. Sakai, H. Ohi, M. Taya, *Biomolecules* **2019**, *9*, 342.
[11] S. Sakai, S. Ito, H. Inagaki, K. Hirose, T. Matsuyama, M. Taya, K. Kawakami, *Biomicrofluidics* **2011**, *5*, 13402.
[12] S. W. Lee, J. Kim, M. Do, E. Namkoong, H. Lee, J. H. Ryu, K. Park, *Acta Biomater.* **2020**, *115*, 275.
[13] K. N. Meadows, P. Bryant, K. Pumiglia, *J. Biol. Chem.* **2001**, *276*, 49289.
[14] T. Roy, B. D. James, J. B. Allen, *Macromol. Biosci.* **2021**, *21*, 2000337.
[15] D. Hanjaya-Putra, V. Bose, Y. I. Shen, J. Yee, S. Khetan, K. Fox-Talbot, C. Steenbergen, J. A. Burdick, S. Gerecht, *Blood* **2011**, *118*, 804.
[16] S. Gerecht, J. A. Burdick, L. S. Ferreira, S. A. Townsend, R. Langer, G. Vunjak-Novakovic, *Proc. Natl. Acad. Sci. USA* **2007**, *104*, 11298.
[17] M. Frye, A. Taddei, C. Dierkes, I. Martinez-Corral, M. Fielden, H. Ortsäter, J. Kazenwadel, D. P. Calado, P. Ostergaard, M. Salminen, L. He, N. L. Harvey, F. Kiefer, T. Makinen, *Nat. Commun.* **2018**, *9*, 1511.
[18] D. Hanjaya-Putra, S. Saha, F. Fan, L. Alderfer, F. Graham, E. Hall, *Biomater. Sci.* **2023**, *11*, 7346.
[19] E. Nyman, F. Huss, T. Nyman, J. Junker, G. Kratz, *J. Plast. Surg. Hand Surg.* **2013**, *47*, 89.
[20] C. C. Termeer, J. Hennies, U. Voith, T. Ahrens, J. M. Weiss, P. Prehm, J. C. Simon, *J. Immunol.* **2000**, *165*, 1863.
[21] X. Pang, W. Li, L. Chang, J. E. Gautrot, W. Wang, H. S. Azevedo, *ACS Appl. Mater. Interfaces* **2021**, *13*, 25792.
[22] W. Mubarok, K. C. M. L. Elvitigala, S. Sakai, *Gels* **2022**, *8*, 387.
[23] K. C. M. L. Elvitigala, W. Mubarok, S. Sakai, *Polymers* **2022**, *14*, 5034.
[24] W. Mubarok, K. C. M. L. Elvitigala, M. Nakahata, M. Kojima, S. Sakai, *Cells* **2022**, *11*, 881.
[25] W. Mubarok, K. C. M. L. Elvitigala, T. Kotani, S. Sakai, *Carbohydr. Polym.* **2023**, *316*, 121026.
[26] R. Tzoneva, V. Uzunova, S. Apostolova, A. Krüger-Genge, A. T. Neffe, F. Jung, A. Lendlein, *Clin. Hemorheol. Microcirc.* **2016**, *64*, 941.
[27] Y. Z. Wang, M. L. Cao, Y. W. Liu, Y. Q. He, C. X. Yang, F. Gao, *Exp. Biol. Med.* **2011**, *236*, 84.

[28] D. Yee, D. Hanjaya-Putra, V. Bose, E. Luong, S. Gerecht, *Tissue Eng., Part A* **2011**, *17*, 1351.
[29] H. Chen, J. Qin, Y. Hu, *Molecules* **2019**, *24*, 617.
[30] X. Li, A. Xu, H. Xie, W. Yu, W. Xie, X. Ma, *Carbohydr. Polym.* **2010**, *79*, 660.
[31] Y. Ni, M. Y. M. Chiang, *Soft Matter* **2007**, *3*, 1285.
[32] J. Xu, M. Sun, Y. Tan, H. Wang, H. Wang, P. Li, Z. Xu, Y. Xia, L. Li, Y. Li, *Differentiation* **2017**, *96*, 30.
[33] M. Sun, G. Chi, P. Li, S. Lv, J. Xu, Z. Xu, Y. Xia, Y. Tan, J. Xu, L. Li, Y. Li, *Int. J. Med. Sci.* **2018**, *15*, 257.
[34] Y. T. Yeh, S. S. Hur, J. Chang, K. C. Wang, J. J. Chiu, Y. S. Li, S. Chien, *PLoS One* **2012**, *7*, e46889.
[35] I. Caon, B. Bartolini, A. Parnigoni, E. Caravà, P. Moretto, M. Viola, E. Karousou, D. Vigetti, A. Passi, *Semin. Cancer Biol.* **2020**, *62*, 9.
[36] H. Jariyal, C. Gupta, A. Srivastava, *Int. J. Biol. Macromol.* **2020**, *160*, 1078.
[37] J. P. Califano, C. A. Reinhart-King, *Cell. Mol. Bioeng.* **2008**, *1*, 122.
[38] L. Alderfer, E. Russo, A. Archilla, B. Coe, D. Hanjaya-Putra, *FASEB J.* **2021**, *35*, e21498.
[39] D. Hanjaya-Putra, J. Yee, D. Ceci, R. Truitt, D. Yee, S. Gerecht, *J. Cell. Mol. Med.* **2010**, *14*, 2436.
[40] E. Ingber, *Circ. Res.* **2002**, *91*, 877.
[41] R. C. Savani, G. Cao, P. M. Pooler, A. Zaman, Z. Zhou, H. M. DeLisser, *J. Biol. Chem.* **2001**, *276*, 36770.
[42] S. Matou-Nasri, J. Gaffney, S. Kumar, M. Slevin, *Int. J. Oncol.* **2009**, *35*, 761.
[43] D. Park, Y. Kim, H. Kim, K. Kim, Y. S. Lee, J. Choe, J. H. Hahn, H. Lee, J. Jeon, C. Choi, Y. M. Kim, D. Jeoung, *Mol. Cells* **2012**, *33*, 563.
[44] D. K. Choi, Y. K. Kim, S. W. Park, H. Lee, S. Lee, S. A. Kim, S. J. Kim, J. Lee, W. Kim, S. H. Min, *Sci. Rep.* **2020**, *10*, 12089.
[45] L. Y. W. Bourguignon, H. Zhu, L. Shao, Y. W. Chen, *J. Biol. Chem.* **2001**, *276*, 7327.
[46] S. J. Kim, S. C. Owen, *Biochim. Biophys. Acta, Biomembr.* **2020**, *1862*, 183348.
[47] S. Sakai, K. Hirose, K. Taguchi, Y. Ogushi, K. Kawakami, *Biomaterials* **2009**, *30*, 3371.
[48] M. Khanmohammadi, S. Sakai, M. Taya, *Int. J. Biol. Macromol.* **2017**, *97*, 308.
[49] M. Hidaka, M. Kojima, M. Nakahata, S. Sakai, *Polymers* **2021**, *13*, 1382.
[50] K. C. M. L. Elvitigala, W. Mubarok, S. Sakai, *Soft Matter* **2023**, *19*, 5880.